

## Precision spectroscopy of Mg atoms in a magneto-optical trap

This content has been downloaded from IOPscience. Please scroll down to see the full text.

2014 Quantum Electron. 44 521

(<http://iopscience.iop.org/1063-7818/44/6/521>)

View [the table of contents for this issue](#), or go to the [journal homepage](#) for more

### Download details:

IP Address: 130.75.103.119

This content was downloaded on 09/11/2016 at 15:30

Please note that [terms and conditions apply](#).

You may also be interested in:

[Optical frequency standards and femtosecond lasers](#)

E V Baklanov and P V Pokasov

[Secondary laser cooling and capturing of thulium atoms in traps](#)

D D Sukachev, E S Kalganova, A V Sokolov et al.

[Celebrating 50 years of the laser \(Scientific session of the general meeting of the Physical Sciences Division of the Russian Academy of Sciences, 13 December 2010\)](#)

[Frequency standards and frequency measurement](#)

A Bauch and H R Telle

[Laser cooling of rare-earth atoms and precision measurements](#)

Nikolai N Kolachevsky

[Realization of the metre by frequency-stabilized lasers](#)

J Helmcke

[Optical frequency standards](#)

Patrick Gill

# Precision spectroscopy of Mg atoms in a magneto-optical trap

A.N. Goncharov, A.E. Bonert, D.V. Brazhnikov, A.M. Shilov, S.N. Bagayev

**Abstract.** We report the results of experimental investigations aimed at creation of the optical frequency standard based on magnesium atoms cooled and localised in a magneto-optical trap (MOT). An experimentally realised MOT for magnesium made it possible to obtain a cloud comprising  $\sim 10^6$ – $10^7$  atoms at a temperature of 3–5 mK. The results of ultra-high resolution spectroscopy of intercombination  $^1S_0$ – $^3P_1$  transition for Mg atom are presented, the resonances in time-domain separated optical fields with the half-width of  $\Gamma = 500$  Hz are recorded, which corresponds to the  $Q$ -factor of the reference line  $Q = \nu/\Delta\nu \sim 1.3 \times 10^{12}$ .

**Keywords:** laser cooling, magnesium, frequency standard.

## 1. Introduction

Frequency standards play an extremely important role both in fundamental research investigations and in various metrological and navigation applications. This is related, first of all, to the fact that modern frequency standards which since 1968 have realised the etalon for a fundamental unit in the SI system – second, are by several orders of magnitude (4–5) more precise than etalons of other physical values. Presently, the primary frequency standard of time is realised in the microwave range ( $\sim 9.2$  GHz) based on a stable transition between sublevels of the hyperfine structure in  $^{133}\text{Cs}$  atom. The international atomic time (TAI) scale is based on this frequency standard. Atomic frequency standards of the microwave range are widely used in navigation systems GPS and GLONASS. The high accuracy of determining coordinates in these navigation systems is mainly related to the stability and accuracy of the frequency standards.

Probably, the relative accuracy of the primary caesium frequency standard has reached its limit. The relative accu-

racy of  $\Delta\nu/\nu \sim 2 \times 10^{-16}$  reached in stationary installations based on a ‘fountain’ of cold caesium atoms is determined by the fundamental physical reasons such as the frequency shifts due to collisions between cold atoms, thermal emission, gravitational shift and so on [1].

A further increase in the accuracy of frequency standards is associated with the transfer from the microwave to the optical range. Frequency references in the optical range are narrow resonances in the absorption spectra of ultra-cold ( $T \sim 1$ – $10$   $\mu\text{K}$ ) single ions and ensembles of neutral atoms localised in electromagnetic and optical traps. Investigations in the field of optical frequency standards have been active in recent decades due to the progress in employing optical frequency synthesisers based on the femtosecond lasers utilising stable mode locking. The employment of femtosecond optical frequency synthesisers gives a possibility of transferring the metrological characteristics of oscillators of the optical range to the radio-frequency range realising in this way the time standard based on a highly stable oscillator of the optical range in a compact form. An important advantage of optical frequency standards as compared to microwave standards is their potentially higher stability of short averaging time (0.1– $10^3$  s), which makes it possible to perform accurate measurements faster.

Experiments on creating optical frequency standards on the basis of cold atoms and ions are performed in leading metrological centres of the world. Presently, most precise are optical standards based on single ions  $\text{Hg}^+$ ,  $\text{Al}^+$ . The accuracy of a  $\text{Hg}^+$  standard is higher than that of the best microwave standards and is equal to  $\Delta\nu/\nu \sim 3 \times 10^{-17}$  [2]. Even more outstanding results have been obtained with  $\text{Al}^+$  ions [3]. The accuracy of frequency standards on neutral alkali-earth atoms (Ca, Sr, Mg) and Yb, Hg cooled and localised in so-called optical lattices [4] is yet worse than that of standards on single ions. In the case of frequency standards on neutral atoms localised in optical lattices as well as in the case of standards on single ions in ion traps, the movement of atoms is limited in space by a fraction of the wavelength which eliminates an influence of Doppler and recoil effects on the position of the line centre of the optical transition – Lamb–Dicke effect [5]. With experimentally realised optical lattices (dipole traps produced by a standing light wave with a specially chosen ‘magic’ wavelength [4]) comprising  $10^3$ – $10^5$  cold atoms the preferential may become standards on neutral atoms which have a better signal/noise ratio and, consequently, provide a higher frequency stability. The highest long-term stability and accuracy of frequency has been demonstrated for ‘lattice’ optical standards on Sr and Yb atoms [6, 7].

The level structure of atoms with the  $ns^2$  valence shell, such as alkaline-earth (Mg, Ca, Sr) atoms, Yb and Hg atoms

**A.N. Goncharov** Institute of Laser Physics, Siberian Branch, Russian Academy of Sciences, prosp. Akad. Lavrent’eva 13/3, 630090 Novosibirsk, Russia; Novosibirsk State University, ul. Pirogova 2, 630090 Novosibirsk, Russia; Novosibirsk State Technical University, prosp. Karla Marksa 20, 630092 Novosibirsk, Russia; e-mail: gonchar@laser.nsc.ru;

**A.E. Bonert** Institute of Laser Physics, Siberian Branch, Russian Academy of Sciences, prosp. Akad. Lavrent’eva 13/3, 630090 Novosibirsk, Russia;

**D.V. Brazhnikov, A.M. Shilov, S.N. Bagayev** Institute of Laser Physics, Siberian Branch, Russian Academy of Sciences, prosp. Akad. Lavrent’eva 13/3, 630090 Novosibirsk, Russia; Novosibirsk State University, ul. Pirogova 2, 630090 Novosibirsk, Russia

Received 3 March 2014; revision received 9 April 2014

*Kvantovaya Elektronika* 44 (6) 521–526 (2014)

Translated by N.A. Raspopov

with the fundamental term  $^1S_0$ , are specific in that there are narrow optical intercombination  $^1S_0 - ^3P_1$  transitions and extremely narrow  $^1S_0 - ^3P_0$  and  $^1S_0 - ^3P_2$  transitions which may be references for stabilising a laser frequency. In addition, spectra of these atoms have strong resonance transitions  $^1S_0 - ^1P_1$  which may provide efficient cyclic interaction with the resonance laser radiation for laser cooling and localisation of atoms in traps. The possibility of employing all mentioned atoms in frequency standards is studied, also the possible creation of the frequency standard based on the transition between fine structure components of the fundamental level of thulium atom is considered [8]. Magnesium atom is also a promising candidate for creating a frequency standard both in optical and in microwave ranges [9–11].

## 2. Magnesium

A schematic diagram of magnesium levels is shown in Fig. 1. In contrast to other alkali-earth atoms, for which laser cooling and localising in magneto-optical traps (MOTs) have been realised, internal electron shells of Mg are filled which may simplify the calculation of influence of various physical factors on frequency shifts of ‘clock transition’ and, in this way, reduce systematic errors of the frequency standard. The relatively small wavelength of the clock transition (457 nm) results in a small frequency shift due to black body radiation (BBR). The value of the BBR shift for magnesium atom is 10 times less than the shift for Sr or Yb atoms [12]. The isotope composition of magnesium (Mg24 – 79%, Mg25 – 10%, Mg26 – 11%) gives the possibility to work with either bosons Mg24, Mg26 having a zero nuclear spin or a fermion Mg25 which has the nuclear spin of 5/2. In creating a frequency standard on Mg atoms, the transition  $^1S_0 - ^3P_1$  with the natural linewidth of 36 Hz and extremely narrow transitions  $^1S_0 - ^3P_2$  and  $^1S_0 - ^3P_0$  seem attractive. In the case where the  $^1S_0 - ^3P_0$  transition in Mg24 is used as a reference line, the method of magneto-induced spectroscopy seems promising [13]. The strong transition  $^1S_0 - ^1P_1$  at the wavelength of 285 nm with the width  $\Gamma = 79$  MHz in magnesium atom is fully closed. The cyclic character of the interaction between resonance radiation and Mg atoms is only limited by their cascade ionisation which leads to losses of atoms at a high intensity of UV cooling radiation [14]. A strong closed transition makes it possible to efficiently control the motion of magnesium atoms by a laser radiation at the wavelength of 285 nm [15] and to efficiently cool and localise atoms in the MOT. In the laser cooling at the resonance transition  $^1S_0 - ^1P_1$  the Doppler limit on temperature  $T_D = h\Gamma/2k_B = 1.9$  mK, where  $h$  is Planck’s constant and  $k_B$  is the Boltzmann constant. The MOT may be loaded with magnesium atoms directly from a thermal beam with no preliminary cooling in a Zeeman slower. The intercombination transition of magnesium atom  $^1S_0 - ^3P_1$  with the natural bandwidth of 36 Hz [16] is attractive for creating a frequency standard. However, the small width of this transition makes it inappropriate for using in a second stage of atom cooling, in contrast to the case of Ca, Sr, Yb, and Hg atoms. The level structure of magnesium atom complicates deep cooling to temperatures down to  $\sim 10$   $\mu$ K which is, along with the high value of the recoil effect  $2\pi\delta = \hbar k^2/2M = 2\pi 39.6$  kHz, a main factor which complicates the employment of magnesium in creation of frequency standards. Realisation of the frequency standard having the relative inaccuracy  $\Delta\nu/\nu = 10^{-16} - 10^{-17}$  requires the sub-Doppler cooling of magnesium atoms. A temperature close to the

‘recoil temperature’ has been obtained while using for laser cooling the transition  $^3P_2 - ^3D_3$  [17]. Calculations show that this transition is appropriate for sub-Doppler cooling in the laser fields with the polarisation gradient [18]. Realisation of sub-Doppler cooling will later allow one to localise atoms in the optical lattice and employ for the frequency standard the strongly forbidden transition  $^1S_0 - ^3P_0$ . Localisation of magnesium atom in the limited space with a dimension shorter than the wavelength will solve the problem of the strong recoil effect and eliminate an influence of the linear Doppler effect.

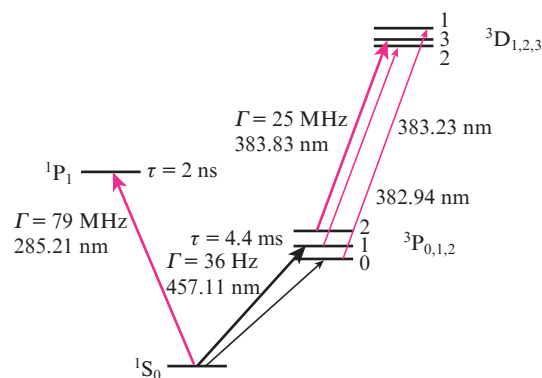


Figure 1. Levels of Mg atom: splitting of  $^3P$  and  $^3D$  levels is magnified.

## 3. Magneto-optical trap

Capturing and cooling of atoms in the MOT is a first stage for obtaining ultra-cold magnesium atoms needed for creating an optical frequency standard. A MOT for magnesium atoms has specific features. Localisation of atoms in the MOT with the strong resonance transition  $^1S_0 - ^1P_1$  having the wavelength of 285.2 nm and the linewidth of 79 MHz requires a strong ( $100 - 150$  G  $\text{cm}^{-1}$ ) gradient of the magnetic field [19]. Windows made of quartz transparent for UV radiation are required for passing the laser radiation into a high-vacuum chamber of the MOT. The high saturated intensity  $I_{\text{sat}} = 440$  mW  $\text{cm}^{-2}$  stipulates the employment of a radiation source at the wavelength of 285 nm with the power of 50–100 mW. A scheme of the MOT for magnesium atoms is shown in Fig. 2.

The high-vacuum MOT chamber is pumped by an NMD-0.16 ion pump down to a residual gas pressure of  $10^{-7}$  Pa\*. Cooling and localisation of atoms in the centre of the quadruple magnetic trap [20] is performed due to the forces of light pressure and friction which arise in the interaction of magnesium atoms with the six beams of laser radiation (three pairs of mutually perpendicular light waves) having corresponding circular polarisations and the frequency detuning from resonance to red wavelengths in a magnetic field with the gradient [21]. The magnetic system of the MOT is formed by two copper coils placed inside a vacuum chamber. The separation between the coils (having the diameter of 20 mm and the cross section  $4 \times 4$  mm) is 8.5 mm. At the current  $I = 150$  A flowing in the coils in opposite directions the gradient

\*The high-vacuum chamber of the MOT was fabricated at the O.P. Pchelyakov Laboratory (Institute of Semiconductor Physics, Siberian Branch, RAS).

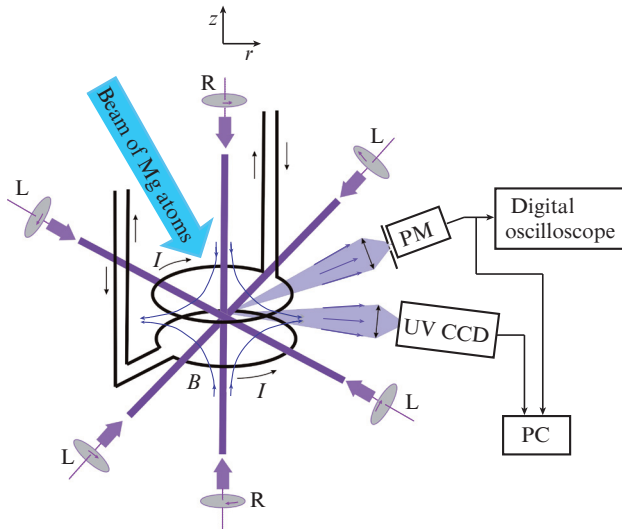


**Figure 2.** Schematic of the magneto-optical trap for magnesium atoms: (PC) computer system for detecting and controlling experiments; (UV CCD) CCD-camera with quartz objective sensitive in the UV spectral range; (L, R) left- and right-polarised radiation beams.

of the magnetic field is  $150 \text{ G cm}^{-1}$  along the  $z$  axes and  $75 \text{ G cm}^{-1}$  in a radial direction  $r$  (see Fig. 2). In the case of unidirectional currents flowing in the coils, a uniform magnetic field is produced in the centre of the MOT. The inductance of the coils with supplying conductors is  $1.1 \mu\text{H}$ . A small value of the inductance provides fast triggering of the magnetic field in time intervals of shorter than  $10 \mu\text{s}$ . The MOT is loaded from the atomic beam which is formed by effusion of atoms through a hole  $0.8 \text{ mm}$  in diameter from the oven with metallic magnesium having the temperature of  $390^\circ\text{C}$ . Atoms are loaded to the MOT from a low-velocity ( $v < 100 \text{ m s}^{-1}$ ) wing of the atom distribution over velocities in the thermal beam. For faster loading, the distance from the source beam to the centre of the MOT should be minimised; in our case, the distance was  $30 \text{ cm}$ .

Localisation and cooling of atoms in the MOT was performed by using  $285\text{-nm}$  radiation of the laser system based on a cw ring R6G dye laser with the following frequency doubling in an external resonator with a BBO nonlinear crystal [15]. At the output of the frequency doubler the radiation power reaches  $100 \text{ mW}$ . The detuning of the radiation frequency from the centre of the absorption line of magnesium atoms on the transition  $^1\text{S}_0 - ^1\text{P}_1$  is controlled by resonances of saturated absorption in the cell filled with magnesium vapour. The optimal detuning was  $-100 \text{ MHz}$ . The cooling laser beams in three mutually orthogonal directions [two pairs in the horizontal plane and one pair in the vertical plane (along the axes of magnetic system)] were formed by two beamsplitters and turning deflecting mirrors. Oncoming waves were created by reflecting the beams passed through the vacuum chamber in a reverse direction by the mirrors. The required circular  $\sigma^+(\text{R})$  and  $\sigma^-(\text{L})$  polarisations of beams were created by six phase plates  $\lambda/4$  (by two for each direction): one plate was placed in front of the chamber and the other was placed in front of a back reflecting mirror. The power of each of the six beams was  $5\text{--}7.5 \text{ mW}$ . At the waist of the laser beam  $w = 2 \text{ mm}$ , the saturation parameter  $S$  for a single beam was  $0.2\text{--}0.3$ . The shape of a cloud of cold atoms in the MOT was recorded with an UV CCD-camera and the signal of fluores-

cence was detected with a photomultiplier (PM). The number of cold atoms in a cloud was estimated by the signal of fluorescence which was calibrated by the fluorescence of the thermal beam of magnesium atoms. Estimates show that a cloud of size of  $0.5 \text{ mm}$  comprises  $10^6\text{--}10^7$  atoms. The temperature of atoms in a cloud determined by the ‘release–capture’ method [22] was equal to  $3\text{--}5 \text{ mK}$ . The lifetime of atoms in the MOT determined by collisions with the residual gas pressure of  $(3\text{--}4) \times 10^{-7} \text{ Pa}$  was  $\sim 15 \text{ s}$ , by collisions with magnesium atoms in the thermal beam – about  $1\text{--}2 \text{ s}$ , and by step ionisation at a maximal power of cooling radiation  $45 \text{ mW}$  (in all the six beams) –  $0.3 \text{ s}$ . The time of MOT loading was  $0.1\text{--}2 \text{ s}$  depending on the power of UV radiation and diameter of cooling beams. The unsaturated absorption of resonance radiation by the cloud of cold atoms was  $\sim 20\%$  which corresponds to the atom concentration at the centre of the cloud  $n_0 \sim 10^{10} \text{ cm}^{-3}$  and is by an order of magnitude less than the concentration at which reabsorption processes produce the repulsive force which limits the concentration of atoms in the MOT [19].

#### 4. Spectroscopy of cold magnesium atoms in the MOT

The natural linewidth of the intercombination transition  $^1\text{S}_0 - ^3\text{P}_1$  of magnesium atom Mg24 at the frequency of  $655 \text{ THz}$  is  $36 \text{ Hz}$ , which is promising for creating a frequency standard. The main limiting factor in this case is the Doppler effect. At a temperature of  $3 \times 10^{-3} \text{ K}$  the Doppler width of the absorption line is  $5.2 \text{ MHz}$ , which is by five orders greater than the homogeneous width of the transition. Even at the atomic temperature equal to the limit determined by the recoil effect  $T_{\text{rec}} = 4.9 \times 10^{-6} \text{ K}$  the Doppler width is  $\Delta\nu_D \sim 200 \text{ kHz}$ . Methods of nonlinear laser spectroscopy make it possible to observe lines without Doppler broadening; however, the residual Doppler effect (for example, due to the curvature of the wave front of laser radiation or inaccuracy of laser beam adjustment in a horizontal plane [23]) results in a shift of the centre of the observed line. For reaching the relative error of the frequency standard of  $10^{-16}$  it is necessary to compensate for the Doppler effect to the degree of  $10^{-7}\text{--}10^{-6}$ . In the frequency standards based on cool free atoms the residual Doppler effect yields the resulting uncertainty of frequency on the order of  $10^{-14}\text{--}10^{-15}$  [23, 24]. Further enhancement of the accuracy of optical frequency standards based on neutral atoms is related to spatial localisation of atoms in optical lattices or with using single ions in ion traps. In a number of applications of optical standards, of principal importance is the frequency stability, which may be substantially higher than the frequency uncertainty. The limiting reachable frequency stability for an averaging time  $\tau$ , which is determined by quantum fluctuations due to a limited number of atoms (quantum projection noise) is characterised by the Allan variance:

$$\sigma_{\text{QPN}}(\tau) = \frac{1}{\pi Q} \sqrt{\frac{T_c}{\tau}} \sqrt{\frac{1}{N_a}}, \quad (1)$$

where  $T_c$  is the cycle duration of measuring the position of the line centre;  $Q$  is the  $Q$ -factor of the spectral line; and  $N_a$  is the number of atoms interacting with the field.

For the ensemble of magnesium atoms ( $N_a = 10^6$ ) the limiting stability determined by quantum statistics may reach  $1.5 \times 10^{-17}/\sqrt{\tau}$  ( $\tau$  is taken in seconds) at the linewidth of  $\sim 100 \text{ Hz}$

( $Q = 6.6 \times 10^{12}$ ) and  $T_c = 10^{-11}$  s. Undoubtedly, for obtaining such frequency stability one should solve the problem of frequency noise of the source of probe laser radiation (Dicke effect [25]). The radiation line may be narrowed to a required value by stabilising the frequency to the transmission band of a high- $Q$  Fabry–Perot interferometer with a low level of thermal noise [26, 27]. At a long averaging time ( $\tau > 10^3$ ), the systematic frequency shifts caused by changes of various physical and technical parameters will contribute into the stability. For studying the systematic relative shifts of frequency on the order of  $10^{-17}$ – $10^{-18}$  the required frequency stability is  $(10^{-17}$ – $10^{-16})/\sqrt{\tau}$  at the time of averaging  $\tau = 10^2$ – $10^3$  s. Employment of the intercombination transition in magnesium for obtaining a high frequency stability at such averaging time is of particular interest.

Investigation of the  $^1S_0$ – $^3P_1$  transition of cold magnesium atoms localised in the MOT was performed by the method of fields separated in time [28]. A cloud of magnesium atoms consecutively interacts with two pairs of the light pulses formed from cw radiation of a highly stable laser system with the radiation wavelength of 457 nm [29] by acousto-optic modulators. A schematic diagram of the experimental setup is shown in Fig. 3.

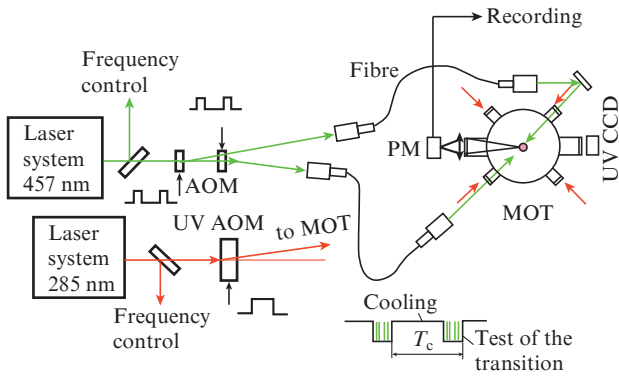


**Figure 3.** Schematic of the experimental setup.

The processes of preparing an ensemble of cold atoms in the MOT and testing a narrow optical transition are separated in time and performed in cycles. The time diagram of the experiment is presented in Fig. 4.

The cycle starts by switching on the UV radiation and the magnetic field gradient for a time of 1–1.5 ms for cooling and capturing cold atoms at the central part of the MOT. This time is substantially shorter than the duration of the initial MOT loading because during the cycle only a negligible part of atoms is lost due to the interaction with probe laser radiation. During the time of switching off the cooling radiation, the other atoms in the cloud have no time to leave the domain of crossing of cooling beams and are again ‘re-captured’. After switching off the UV radiation and magnetic field gradient, a uniform magnetic field is switched on in the MOT by changing the current in coils of the magnetic system to unidirectional mode. The magnetic field magnitude at the coil current of 30 A is  $\sim 25$  G which detunes the frequencies of  $\sigma^+$  and  $\sigma^-$  components of the  $^1S_0$ – $^3P_1$  transition by approximately 50 MHz relative to the frequency of  $\pi$ -transition with  $\Delta m = 0$ , for which the linear Zeeman effect is absent. The quadratic Zeeman effect causes the frequency of the transition with

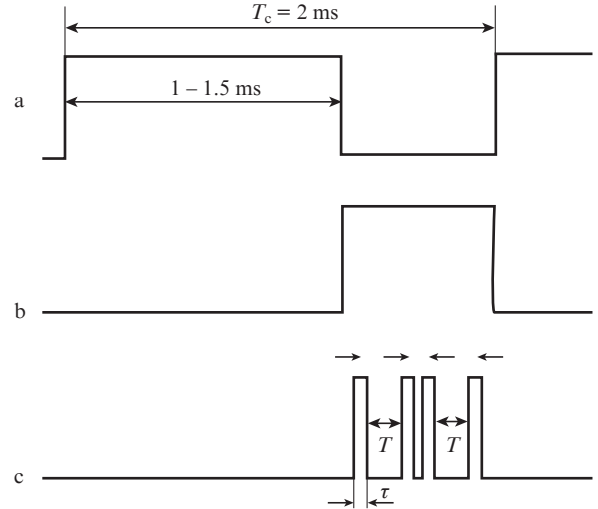


**Figure 4.** Time diagram of the experiment: (a) gradient of the magnetic field and UV radiation, (b) uniform magnetic field and (c) probe field at the wavelength of 457 nm (two pairs of pulses in opposite directions).

$\Delta m = 0$  to shift by  $\sim 1$  kHz (the coefficient of the quadratic Zeeman effect is  $1.6 \text{ Hz G}^{-2}$ ). For creating the frequency standard with the relative error of less than  $10^{-16}$  it is necessary to reduce the magnetic field to approximately 5 G and to control it with a relative inaccuracy of less than  $10^{-3}$ . In 20  $\mu\text{s}$  after switching on the uniform magnetic field, the light pulses of probe radiation with the wavelength of 457 nm formed by acousto-optic modulators are directed to the MOT through two single-mode polarisation-maintaining fibres: two pulses from one side and two pulses from the opposite side. The waists of laser beams in the MOT are  $w_0 = 2$  mm, pulse durations are  $\tau = 5 \mu\text{s}$ , which corresponds to the Rabi excitation angle  $\Omega_R \tau = \pi/2$  ( $\pi/2$ -pulse) at the laser beam power  $\sim 25$  mW. At such pulse durations the corresponding spectral width is  $\sim 100$  kHz. The Doppler width of the absorption line for the ensemble of atoms having the temperature of 3 mK is 5 MHz. Thus, only 1/50 part of atoms from the cloud interacts with laser radiation. The part of atoms interacting with the field may be substantially enlarged by cooling the atoms to a temperature of  $\sim 10 \mu\text{K}$ . The time delay between the pairs of pulses was chosen 20  $\mu\text{s}$ . In the interaction of atoms with four time-separated laser pulses, the observed signal is in the best way described in terms of atomic interferometry [30] and the probability for an atom to transfer to the excited state  $^3P_1$  is described by the expression

$$P(\Delta) = A(\Delta) \{ \cos[2T_{\text{eff}}(\Delta - \delta) + \phi_{1234}] \} + B(\Delta) \cos[2T_{\text{eff}}(\Delta + \delta) + \phi_{1234}] + P_{\text{neg}}(\Delta), \quad (2)$$

where  $\Delta = \nu_{\text{las}} - \nu_0$  is the detuning of laser radiation from the transition frequency;  $\delta$  is the recoil frequency;  $T_{\text{eff}} = (4/\pi)\tau + T$  is the effective time between pulses;  $\phi_{1234} = \phi_2 - \phi_1 + \phi_4 - \phi_3$  is the phase difference of the laser fields of pulses at the point of interaction with an atom; and  $P_{\text{neg}}(\Delta)$  is determined by the incoherent part of atom interaction with field. The first two terms in the right-hand side of (2) describe the interference signals, i.e., the Ramsey–Borde resonances at the output of two interferometers corresponding to two components of recoil doublet with the amplitudes  $A(\Delta)$  and  $B(\Delta)$ , the third

term describes the incoherent part of interaction with the characteristic linewidth determined by the Doppler effect and having a Lamb dip at its centre. The characteristic spectral width of amplitude functions  $A(\Delta)$  and  $B(\Delta)$  corresponds to the spectral width of a light pulse  $\sim 100$  kHz. In the cases where the delay between the pairs of pulses is substantially shorter than the time of atom coherent interaction with the field, or where the interaction time is substantially shorter than the relaxation time of the excited level, the amplitudes of recoil doublet components are equal  $A(\Delta) = B(\Delta)$ ; it is just the case realised in our experiment. At a longer delay between pulses  $T$  the spectral resolution of the experiment increases and the period of Ramsey fringes reduces  $\Delta\nu_{\text{FR}} = 1/2T_{\text{eff}}$ . A constructive addition of interference fringes from the recoil doublet components requires fulfilment of the condition  $\Delta\nu_{\text{FR}}N = 2\delta$ , where  $N$  is an integer. The signal detected in our experiment (resonance fluorescence of atoms on the transition  $^1S_0-^1P_1$ ) is proportional to a population of the fundamental state  $^1S_0$ . Excitation of atoms to the  $^3P_1$  state causes the detected signal to fall. In the transfer of a single atom to the  $^3P_1$  state the number of fluorescence photons per second may change by as much as  $10^8-10^9$ ; the noticeable signal amplification occurs [31]. In this case, photon quantum noise makes no substantial contribution into the results of measurements; the main source of noise is fluctuation of the number of atoms interacting with the field.

Detection of narrow Ramsey resonances requires the source of radiation with a narrow generation line. In our case the source with  $\lambda = 457$  nm was a Ti:sapphire laser ( $\lambda = 914$  nm) combined with a frequency doubler on a  $\text{KNbO}_3$  crystal in an external resonator [29]. Usually, the radiation power at the wavelength of 457 nm was 100 mW. The narrow generation line was provided by a two-stage system of frequency stabilisation with employment of two highly stable Fabry–Perot interferometers. The first interferometer with the coefficient of finesse  $F = 600$  and free spectral range  $\text{FSR} = 300$  MHz was made of invar and provided the preliminary narrowing of the generation line of the Ti:sapphire laser, the second (zero-dur) interferometer ( $F = 10^5$ ,  $\text{FSR} = 375$  MHz) was used for correcting low-frequency perturbations of the first interferometer through automatic adjustment of its length by the piezoelectric actuator with an interferometer mirror installed on it. The radiation passed to the second interferometer through a two-pass AOM which was used for tuning the radiation frequency of the clock laser system. Both the interferometers were placed into vacuum chambers and thermally stabilised. Isolation from vibrations was provided by a Minus K 100 BM-4 vibration isolation table (the first interferometer) and spring suspension system (the second interferometer). The frequency band of processing perturbations in the Ti:sapphire laser was 200 kHz, which provided less than 100-Hz width for the radiation line at  $\lambda = 457$  nm. The frequency drift of stabilised laser radiation  $\sim 1$  Hz  $\text{s}^{-1}$  is related to ageing of the base material in the second interferometer.

In recording narrow resonances, the radiation frequency of the laser system was tuned by a frequency synthesiser, the signal from which controlled AOM in the frequency stabilising system of the second interferometer. The fluorescence signal from a cloud of cold magnesium atoms on the resonance transition with  $\lambda = 285$  nm was detected by the PM.

The Ramsey–Borde resonances in time-separated fields are shown in Fig. 5a for the delays between pulses  $T = 7.5, 58, 102, 210$   $\mu\text{s}$  corresponding to  $N = 2, 10, 17, 33$ . The Ramsey fringes at  $T = 246$   $\mu\text{s}$  ( $N = 40$ ) are presented in Fig. 5b. The

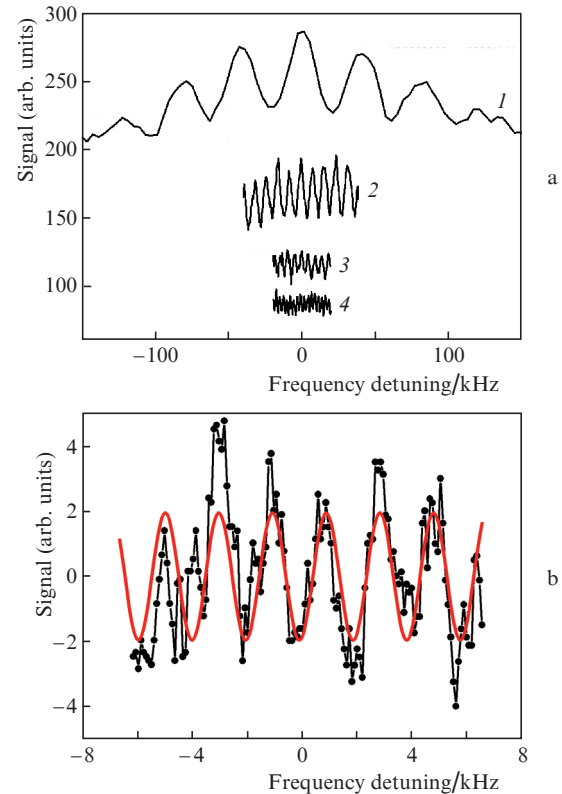


**Figure 5.** (a) Resonances in time-separated fields for the delays between pulses  $T = (1)$  7.5, (2) 58, (3) 102 and (4) 201  $\mu\text{s}$  and (b) Ramsey fringes at  $T = 246$   $\mu\text{s}$ : solid curve is the approximation by the sinusoidal function  $2\sin(2\pi\Delta/1.95)$  with the period of 1.95 kHz and the half-width (HWHM) of 500 Hz; direct records of resonances per single scan are presented, 200 points per record at the averaging time of 0.1 s for each point.

fringe half-width is  $\Gamma = 500$  Hz, which corresponds to the  $Q$ -factor of line  $Q = 1.3 \times 10^{12}$ .

The shift of the central fringe in Fig. 5a relative to the position of the central fringe in Fig. 5b is explained by a frequency drift of the reference interferometer.

The time-of-flight broadening of resonances in the experimental conditions is  $\Gamma_{\text{tof}} = 1.2v/(2\pi d) = 140$  Hz, where  $v$  is the velocity of atoms in the MOT, and  $d$  is the diameter of the laser beam. The signal/noise ratio in the experiment is determined by technical reasons which cause fluctuations of the number of atoms captured in the MOT. This ratio may be substantially increased by cooling the cloud of atoms to a temperature of  $\sim 10$   $\mu\text{K}$ , which is possible under the sub-Doppler cooling of atoms in the triplet transition  $^3P_2 \rightarrow ^3D_3$  at the wavelength of 383.8 nm. If such cooling is performed, magnesium atoms are localised in a ‘triplet’ MOT, and detection of the population of level  $^3P_1$  may be performed through a cyclic transition  $^3P_2 \rightarrow ^3D_3$  without a background signal, in contrast to the case of detection on the  $^1S_0-^1P_1$  transition, which can also substantially increase the ratio signal/noise.

## 5. Conclusions

The possibility of employing cold magnesium atoms localised in the MOT for obtaining the narrow reference lines with a  $Q$ -factor  $Q > 10^{12}$  in creating the optical frequency standard is shown. Presently, we investigate fre-

quency stabilisation on the central fringe of observed resonances. The expected relative frequency instability  $\sigma(\tau)$  is estimated as  $(10^{-13} - 10^{-14})/\sqrt{\tau}$  ( $\tau$  in seconds). A substantial increase in the stability and accuracy of the magnesium frequency standard  $\Delta\nu/\nu$  up to  $10^{-16} - 10^{-17}$  will be possible under cooling atoms to  $\sim 10$   $\mu$ K and their localisation in an optical lattice at a ‘magical’ wavelength [32]. We develop the required sources of laser radiation with the wavelengths of 382.9, 383.3, and 383.8 nm based on semiconductor lasers with frequency doubling for sub-Doppler cooling of Mg atoms on the  $^3P_2 \rightarrow ^3D_3$  transition.

**Acknowledgements.** The work was supported by the Russian Foundation for Basic Research (Grant No. 12-02-00403-a), the Presidium of the Siberian Branch of the Russian Academy of Sciences, and the Presidium of the Russian Academy of Sciences (Extreme Light Fields and Their Applications and Quantum Mesoscopic and Unordered Structures Programmes).

## References

- Parker T.E. *Metrologia*, **47**, 1 (2010).
- Rosenband T. et al. *Science*, **319**, 1808 (2008).
- Chou C.W., Hume D.B., Koelmeij J.C.J., Winelan D.J., Rosenband T. *Phys. Rev. Lett.*, **104**, 070802 (2010).
- Katori H., Takamoto M., Pal’chikov V.G., Ovsyannikov V.D. *Phys. Rev. Lett.*, **91**, 173005 (2003).
- Dicke R.H. *Phys. Rev.*, **89**, 472 (1953).
- Bloom B.J., Nicholson T.L., Williams J.R., Campbell S.L., Bishof M., Zhang X., Zhang W., Bromley S.L., Ye J. doi:10.1038/nature12941 (2014).
- Hinkley N., Sherman J.A., Phillips N.B., Schioppo M., Lemke N.D., Beloy K., Pizzocaro M., Oates C.W., Ludlow A.D. *Science*, **341**, 1215 (2013).
- Kolachevsky N.N. *Usp. Fiz. Nauk*, **181**, 896 (2011) [*Phys. Usp.*, **54**, 863 (2011)].
- De Marchi A., Bava E., Godone A., Giusfredi G. *IEEE Transac. Instrum. Measur.*, **IM-32**, 191 (1983).
- Beverini N., Maccioni E., Strumia F. *Laser Phys.*, **4**, 2 (1994).
- Keupp J., Douillet A., Mehlstaubler T.E., Rehbein N., Rasel E.M., Ertmer W. *Europ. Phys. J. D*, **36**, 289 (2005).
- Porsev S.G., Derevianko A. *Phys. Rev. A*, **74**, 020502 (2006).
- Taichenachev A.V., Yudin V.I., Oates C.W., Hoyt C.W., Barber Z.W., Hollberg L. *Phys. Rev. Lett.*, **96**, 083001 (2006).
- Madsen D.N., Thomsen J.W. *J. Phys. B: At. Mol. Opt. Phys.*, **35**, 2173 (2002).
- Bagayev S.N., Baraulia V.I., Bonert A.E., Goncharov A.N., Seydaliyev M.R., Tychkov A.S. *Laser Phys.*, **11**, 1178 (2001).
- Hansen P.L., Therkildsen K.T., Malossi N., Jensen B.B., van Ooijen E.D., Brusch A., Müller J.H., Hald J., Thomsen J.W. *Phys. Rev. Lett.*, **77**, 062502 (2008).
- Riedmann M., Kelkar H., Wubbena T., Pape A., Kulosa A., Zipfel K., Fim D., Ruhmann S., Friebe J., Ertmer W., Rasel E. *Phys. Rev. A*, **86**, 043416 (2012).
- Brazhnikov D.V., Bonert A.E., Goncharov A.N., Taichenachev A.V., Tumaikin A.M., Yudin V.I., Basalaev M.Yu., Il’enkov R.Ya., Shilov A.M. *Vestnik NGU. Ser. Fiz.*, **7**, 6 (2012).
- Loo F.Y., Brusch A., Sauge S., Allegrini M., Arimondo E., Andersen N., Thomsen J.W. *J. Opt. B: Quantum Semiclass. Opt.*, **6**, 81 (2004).
- Bergemann T., Erez G., Metcalf H. *J. Phys. Rev. A*, **35**, 1535 (1987).
- Raab E.L., Prentiss M., Cable A., Chu S., Pritchard N. *Phys. Rev. Lett.*, **59**, 2631 (1987).
- Chu S., Hollberg L., Bjorkholm J.E., Cable A., Ashkin A. *Phys. Rev. Lett.*, **55**, 48 (1985).
- Friebe J., Riedmann M., Wubbena T., Pape A., Kelkar H., Ertmer W., Terra O., Sterr U., Weyers S., Grosche G., Schnatz H., Rasel E.M. *New J. Phys.*, **13**, 125010 (2011).
- Degenhardt C., Stoehr H., Lisdat C., Wilpers G., Schnatz H., Lipphardt B., Nazarova T., Pottie P., Sterr U., Helmcke J., Riehle F. *Phys. Rev. A*, **72**, 062111 (2005).
- Santarelli G., Audoin C., Makdissi A., Laurent P., Dick G.J., Clairon A. *IEEE Trans. Ultrason. Ferroelectr. Freq. Control*, **45**, 887 (1998).
- Kessler T., Hagemann C., Grebing C., Legero T., Sterr U., Riehle F., Martin M. J., Chen L., Ye J. *Nat. Photon.*, **6**, 687 (2012).
- Swallows M.D., Martin M.J., Bishof M., Benko C., Lin Y., Blatt S., Rey A.M., Ye J. *IEEE Trans. Ultrason. Ferroelectr. Freq. Control*, **59**, 416 (2012).
- Sengstock K., Sterr U., Hennig G., Bettermann D., Müller J.H., Ertmer W. *Opt. Commun.*, **103**, 73 (1993).
- Bagayev S.N., Baraulia V.I., Bonert A.E., Goncharov A.N., Seidaliyev M.R., Farnosov S.A. *Kvantovaya Elektron.*, **31**, 495 (2001) [*Quantum Electron.*, **31**, 495 (2001)].
- Bordé C. *J. Phys. Lett. A*, **140**, 10 (1989).
- Sengstock K., Sterr U., Hennig G., Bettermann D., Müller J.H., Ertmer W. *Opt. Commun.*, **103**, 73 (1993).
- Ovsyannikov V.D., Pal’chikov V.G., Katori H., Takamoto M. *Kvantovaya Elektron.*, **36**, 3 (2006) [*Quantum Electron.*, **36**, 3 (2006)].